Purdue University
Purdue e-Pubs

International Refrigeration and Air Conditioning Conference

School of Mechanical Engineering

2018

Film Rupture And Partial Wetting Over Flat Surfaces

Niccolo Giannetti
niccolo@aoni.waseda.jp

Piyatida Trinuruk
King Mongkut's University of Technology Thonburi, Department of Mechanical Engineering, Thung-khru, Bangkok 10140, Thailand, piyatida.tri@mail.kmutt.ac.th

Seiichi Yamaguchi
Waseda University, Department of Applied Mechanics and Aerospace Engineering, 3-4-1 Okubo, Shinjuku-ku, Tokyo 169-8555, Japan, sei_yamaguchi@aoni.waseda.jp

Kiyoshi Saito
Waseda University, Department of Applied Mechanics and Aerospace Engineering, 3-4-1 Okubo, Shinjuku-ku, Tokyo 169-8555, Japan, saitowaseda@gmail.com

Film Rupture and Partial Wetting over Flat Surfaces

Niccolò GIANNETTI[1]*, Piyatida TRINURUK[2], Seiichi YAMAGUCHI[1], Kiyoshi SAITO[1]

[1] Waseda University, Department of Applied Mechanics and Aerospace Engineering,
3-4-1 Okubo, Shinjuku-ku, Tokyo 169-8555, Japan
Tel/Fax: +81-3-5286-3259

[2] King Mongkut's University of Technology Thonburi, Department of Mechanical Engineering,
Thung-khru, Bangkok 10140, Thailand
Tel:+66 2470 9114, Fax: +66 2470 9111

* Corresponding Author

ABSTRACT

The principle of minimizing the energy of a given stream-wise section of the film is applied in order to investigate the film stability and the local variation of the wetting behavior under an imposed fluid distribution width. The evolution to the stable rivulet configuration is estimated considering the energy of the system under a Lagrangian approach. The Lagrange equation is written with reference to a single generalized wetting coordinate and its time derivative, under the effect of Rayleigh's dissipation function and a generalized force associated to a scalar potential defined as the energy excess with respect to the local energy minimum of the stable rivulet configuration. This methodology is extended to include the hysteresis behavior of the contact angle and wettability hysteresis when increasing or decreasing mass flow rates are delivered. Finally, a first qualitative and quantitative validation of the results is presented with reference to the visual data captured on a dedicated experimental test section.

1. INTRODUCTION

Various heat and mass exchange devices uses thin liquid films as the transfer media for increase the effectiveness and reduce the size of these devices. Several corresponding technical circumstances require conditions that prevent thin liquid films from breaking into a series of rivulets, leaving the solid surface partly uncovered and lowering the extension of the liquid free interface. What is needed is both a criterion for the stability of the film to identify the minimum flow rate able to ensure the complete wetting of the surface and, after the film rupture, a method to estimate the wet (active) part of the same surface, as well as the extension of the free interface for mass transfer. At low Reynolds and high Weber numbers, the assumptions of a film with uniform thickness and complete wetting of the transfer surface cannot be considered, even approximately, rigorous, hence, leading to unacceptable inaccuracy of simulation results of the transfer performance in that operative region. Accordingly, the inadequacy of a recurrent simplifying assumption introduced in previous theoretical models of these devices, namely the assumption of complete wetting, has been widely recognized. Regarding, for instance, falling film absorbers or liquid desiccant contactors, partial wetting of the exchange brings about a reduction of the area of the heat and mass transfer interfaces (Giannetti et al., 2017 [1]; Giannetti et al., 2018 [2]; Varela et al., 2018 [3]). The circumstances under which the film breaks down and the extension of the resulting dry patches are of critical importance to predict the effectiveness of these devices, as well as the efficiency of the system they belong to. However, a general agreement on the precise mechanism of film rupture has not been reached and related data on a variety of influent parameters are incomplete (Maron et al., 1982 [4], N. Brauner et al., 1985 [5]).
As they provide a simple variational method to solve complex, multi-variable physical problems, extremum principles have led to critical results in theoretical as well as technical research areas (Bertola and Cafaro, 2008 [6]), and remain central in modern physics and engineering. In this context, and with regard to the previously stated technical aim, the principle of minimizing the energy of a given stream-wise section of the film is applied in order to

model and investigate the film stability and the local evolution of the wetting behavior under an imposed fluid distribution width. In Mikielewicz and Moszynski (1976) [7] and Giannetti et al. (2016) [8] the rivulet cross-sectional shape is assumed to be a segment of a circle and the distance between adjacent rivulets λ results from the calculation and cannot be set as a geometrical parameter of the problem. Thus, for a fixed width of the solid surface, the assumption of a circular rivulet requires the contact angle to change with varying rivulet size (Doniec, 1988 [9]). Within the bounds of this method, Doniec (1991) [10] uses the variational calculus to determine the rivulet shape, defined the minimum total energy. The solution for a symmetric rivulet is composed of a segment of a straight line and an integral curve that cuts the solid surface with an angle matching the contact angle. In this way, by introducing an additional degree of freedom for the rivulet geometry, the surface width can be used as a parameter.
This study establishes a criterion for defining the film stability for a composite rivulet cross-section shape; this is suitable for predicting the transient evolution of the wetting ability under an imposed fluid distribution width. The evolution from uniform film to the stable rivulet configuration is estimated considering the energy of the system under a Lagrangian approach. The Lagrange equation is written with reference to a single generalized wetting coordinate and its time derivative, under the effect of Rayleigh's dissipation function and a generalized force associated to a scalar potential defined as the energy excess with respect to the local energy minimum of the stable rivulet configuration. Furthermore, this methodology is extended to include the hysteresis behavior of the contact angle (considering advancing and receding values) and wettability hysteresis when gradually increasing or decreasing flow rates are delivered. Finally, a first qualitative and quantitative validation of the results is presented with reference to the visual data captured on a dedicated experimental test section.

2. PHYSICAL MODEL

The first part of the problem (section 2.1) can be synthetized as the identification of the flow transition between two flow-configurations under analysis (schematically represented in Figure 1). Afterwards (in section 2.2), the transient evolution of the phase interfaces under an imposed fluid distribution width is modeled and estimated. This provides information of critical importance for predicting the performance of falling film transfer devices.

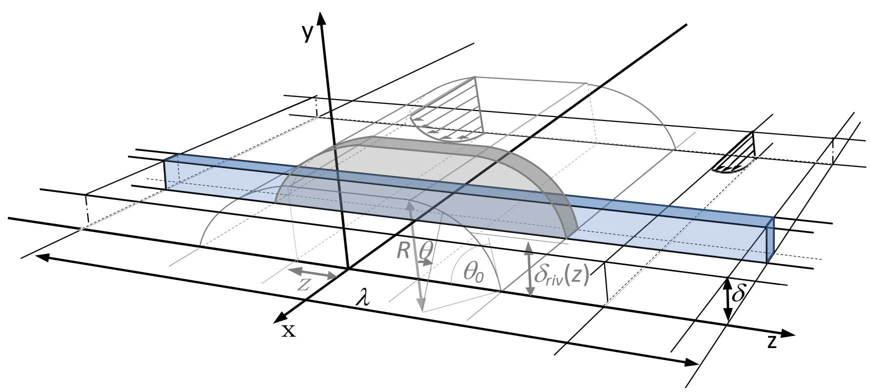

Figure 1: Schematic of rivulet configuration

2.1 Film Stability

The modeling method hereby applied is based on the definition of the ideal geometry (Figure 1) of two flow configurations (a film with uniform thickness fully wetting the solid surface and a rivulet with a composed circular-flat cross-section shape), the solution of the stream-wise momentum equation under the assumptions of Nusselt integral theory (Eq. 1), and the variational method of minimum energy (Mikielewicz and Moszynski (1976) [7]) to predict the rivulet wettability *X* (Eq. 2) and the limit of stability of the uniform film (Eq. 3).

$$\mu\frac{\partial^2 u}{\partial y^2} = -\rho g \tag{1}$$

$$\frac{\partial E_{riv}}{\partial X} = 0, \quad \frac{\partial^2 E_{riv}}{\partial X^2} > 0 \tag{2}$$

$$E_{riv} = E_{uf} \tag{3}$$

A laminar fully developed, homogeneous Newtonian liquid film of uniform thickness δ_u, with uniform surface tension σ (Marangoni effect is not accounted for) and density ρ, flows, wave-less, down over a flat solid wall of width λ (Figure 1), with generic inclination β, only driven by gravity g; it is postulated that each parameter undergoes quasi-static variations;
To use the principle of minimum energy, and define the stable configuration of the rivulet, its total mechanical energy (kinetic energy E_K plus surface tension energy E_σ, Eq. 4) is to be computed, minimized with respect to the geometrical parameter representing for the transversal extension of the rivulet, and lastly compared to the uniform film configuration (Figure 1).

$$E = E_K + E_\sigma = \int_A \frac{1}{2}\rho u^2 dA + \int_S \sigma dS = \int_A \frac{1}{2}\rho u^2 dA + \int_{Slv} \sigma_{lv} dS + \int_{Sls} \sigma_{ls} dS + \int_{Ssv} \sigma_{sv} dS \tag{4}$$

Furthermore, under the same assumptions of Nusselt integral solution for an isothermal plate, the velocity profile and the corresponding film thickness are expressed as in Eqs. 5 and 6.

$$u = \frac{\rho g}{\mu}\sin\beta\left(\delta_u y - \frac{1}{2}y^2\right) \tag{5}$$

$$\delta_u = \left(\frac{3\mu\Gamma}{\rho^2 g \sin\beta}\right)^{1/3} \tag{6}$$

The rivulet cross-section profile $\delta_{riv}(z)$ expressed by Eq. 7 is a symmetrical and continuous combination of a straight segment of a horizontal line and a circular segment, cutting the solid surface with an angle equivalent to the contact angle (Figure 1).

$$\delta_{riv}(z) = \begin{cases} R(\cos\theta - \cos\theta_0), & z \in \langle Z, Z + 2R\sin\theta_0 \rangle \\ R(1-\cos\theta_0), & z \in \langle 0, Z \rangle \end{cases} \tag{7}$$

Considering the rivulet cross-section identified on a plane perpendicular to the flow direction x, and dividing it into thin bands dz of height $\delta_{riv}(z)$, the velocity distribution $u(y,z)$ in such a band is assumed to match the velocity profile in a film of uniform thickness δ_u equal to $\delta_{riv}(z)$. Accordingly, the total energy per unit length λ and unit stream-wise length of the flow dx is expressed, for the uniform film and the rivulet configurations, by Eqs. 8 and 9, respectively.

$$e_u = \frac{\rho}{\lambda}\int_0^{\delta_u} u^2(y)dy + \sigma_{sl} + \sigma_{lv} \tag{8}$$

$$e_{riv} = \frac{2\rho}{\lambda}\int_Z^{Z+R\sin\theta_0}\int_0^{\delta_{riv}} u^2(y)dzdy + \frac{2\rho Z}{\lambda}\int_0^{\delta_{riv}} u^2(y)dy + \sigma_{sv}(1-X) + \sigma_{sl}X + \frac{2\sigma_{lv}}{\lambda}(R\theta_0 + Z) \tag{9}$$

Considering the hydrodynamics of the system (Eq. 5), the energy and the corresponding mass flowrate per unit length Γ are given by Eqs. 10-11.

$$e_u = \frac{1}{15}\frac{\rho^3 g^2 \sin^2\beta}{\mu^2}\delta_u^{\,5} + \sigma_{sl} + \sigma_{lv} \tag{10}$$

$$\Gamma = \int_0^{\delta_u} \rho u(y)dy = \frac{1}{3}\frac{\rho^2 g\sin\beta}{\mu}\delta_u^{\,3} \tag{11}$$

When the film rupture into rivulets occurs, the basic parameter to compute the wet part of the tube surface X (Eq. 12) is the ratio of the rivulet chord at its base to the corresponding width λ of the uniform film; the corresponding mass flow rate per unit width for the rivulet configuration is given by Eq. 13.

$$X = \frac{2R\sin\theta_0 + 2Z}{\lambda} \tag{12}$$

$$\Gamma_{riv} = 2\left[\frac{\rho}{\lambda}\int_{Z}^{Z+R\sin\theta_0}\int_{0}^{\delta_{riv}} u(y)dzdy + \rho\frac{Z}{\lambda}\int_{0}^{\delta_{riv}} u(y)dy\right] = \frac{2}{3}\frac{\rho^2 g\sin\beta}{\lambda\mu}R^3\left[Rf(\theta_0) + Z(1-\cos\theta_0)^3\right] \tag{13}$$

Where, as in Mikielewicz and Moszynski (1976) [7],

$$f(\theta_0) = \int_{0}^{\theta_0}(\cos\theta - \cos\theta_0)^3\cos\theta d\theta = -\frac{1}{4}\cos^3\theta_0\sin\theta_0 - \frac{13}{8}\cos\theta_0\sin\theta_0 - \frac{3}{2}\theta_0\sin^2\theta_0 + \frac{15}{8}\theta_0 \tag{14}$$

The combination of the mass balance between the two configurations and the definition of the wetting ratio X (Eq. 12) yields to Eq. 15, which relates the rivulets radius R to the uniform film thickness δ_u and X; the Young-Dupree equation (Eq. 16) assures the equilibrium of the surface tension forces at the point of contact of the three phases.

$$\left(\frac{\delta_u}{R}\right)^3 = 2\frac{Rf(\theta_0)}{\lambda} + \left(X - \frac{2R\sin\theta_0}{\lambda}\right)(1-\cos\theta_0)^3 \tag{15}$$

$$\sigma_{sv} = \sigma_{sl} + \sigma_{lv}\cos\theta_0 \tag{16}$$

Accordingly, the energy e_{riv} per unit stream-wise length dx and width λ (Eq. 17) is a function of the rivulet radius R.

$$\begin{aligned} e_{riv} = {} & \frac{1}{15}\frac{\rho^3 g^2\sin^2\beta}{\mu^2}R^5\left\{2\frac{R}{\lambda}\psi(\theta_0) + \left[\left(\frac{\delta_u}{R}\right)^3 - \frac{2Rf(\theta_0)}{\lambda}\right](1-\cos\theta_0)^2\right\} + \sigma_{sl} + \\ & + \sigma_{lv}\left\{\left[\frac{\lambda\delta_u{}^3 - 2R^4 f(\theta_0)}{R^3\lambda(1-\cos\theta_0)^3} + \frac{2R\sin\theta_0}{\lambda}\right](1-\cos\theta_0) + \cos\theta_0 + \frac{2}{\lambda}R(\theta_0 - \sin\theta_0)\right\} \end{aligned} \tag{17}$$

Where,

$$\begin{aligned} \psi(\theta_0) &= \int_0^{\theta_0}(\cos\theta - \cos\theta_0)^5\cos\theta d\theta \\ &= \theta_0\left(\frac{5}{16} + \frac{15}{4}\cos^2\theta_0 + \frac{5}{2}\cos^4\theta_0\right) - \sin\theta_0\left(\frac{113}{48}\cos\theta_0 + \frac{97}{24}\cos^3\theta_0 + \frac{1}{6}\cos^5\theta_0\right) \end{aligned} \tag{18}$$

The rivulet will be stable if e_{riv} shows a local minimum with respect to the rivulet radius R (which uniquely determines the wetting ratio X, according to Eq. 15), when X<1. Contrarily, if the rivulet configuration shows no minimum with respect to X, or if the uniform film configuration exhibits a lower value of total energy, the uniform film is stable. Hence, by differentiating Eq. 17 with regard to R, and solving for R once equated to zero (Eq. 19), is possible to establish the geometry of the rivulet in the previously defined stable condition (Eqs. 12 and 15).
The critical condition where the film rupture occurs is related to a minimum value of the film thickness δ_b, which is dependent upon the liquid characteristics in terms of thermo-physical properties, contact angle of the solid-liquid pair, width λ and inclination β of the plain surface. The solution of the system of Eqs. 19-20 gives the critical condition for the uniform film once numerically solved with respect to R_b and δ_b.

$$\frac{\rho^3 g^2 \sin^2\beta}{\mu^2}\left[\frac{4}{5}\frac{R^5}{\lambda}\psi(\theta_0)+\frac{2}{15}\delta_u^{\ 3}R(1-\cos\theta_0)^2-\frac{4}{5}\frac{R^5}{\lambda}f(\theta_0)(1-\cos\theta_0)^2\right]+$$
$$+\sigma_{lv}\left\{\left[-\frac{3\delta_u^{\ 3}}{R^4}\frac{1}{(1-\cos\theta_0)^3}-\frac{2f(\theta_0)}{\lambda(1-\cos\theta_0)^3}+\frac{2\sin\theta_0}{\lambda}\right](1-\cos\theta_0)+\frac{2}{\lambda}(\theta_0-\sin\theta_0)\right\}=0 \tag{19}$$

$$\frac{1}{15}\frac{\rho^3 g^2\sin^2\beta}{\mu^2}\left\langle \delta_b^{\ 5}-R_b^{\ 5}\left\{2\frac{R_b}{\lambda}\psi(\theta_0)+\left[\left(\frac{\delta_b}{R_b}\right)^3-\frac{2R_b f(\theta_0)}{\lambda}\right]R_b^{\ 5}(1-\cos\theta_0)^2\right\}\right\rangle=$$
$$\sigma_{lv}\left\langle\left\{\left[\frac{\lambda\delta_b^{\ 3}-2R_b^{\ 4}f(\theta_0)}{R_b^{\ 3}\lambda(1-\cos\theta_0)^3}+\frac{2R_b\sin\theta_0}{\lambda}\right](1-\cos\theta_0)+\cos\theta_0+\frac{2}{\lambda}R_b(\theta_0-\sin\theta_0)\right\}-1\right\rangle \tag{20}$$

As a result, when the thickness of the uniform film is lowered below the minimum critical thickness ($\delta_u \le \delta_b$), the film is assumed to break into a rivulet with local wetting ratio X (calculated according to Eqs. 15 and 19).

Table 1: Calculation results

	δ_b [m]	θ_0[rad]	X_b	R_b[m]	$e_{riv,b}$[J·m^{-2}]
Mikielewicz and Moszynski (1976) [7]	0.00026	0.99	0.36	0.0010	0.0792
Present work	0.00035	0.99	0.93	0.00079	0.113

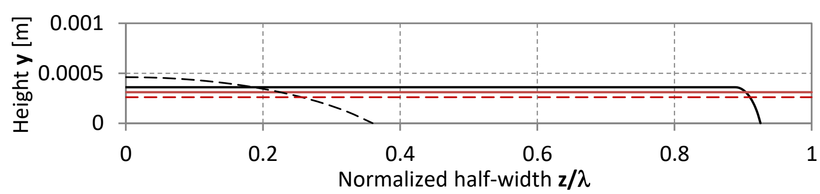

Figure 2: Critical condition [mm] for a uniform film: from Mikielewicz and Moszynski (1976) [7] (continuous lines), this study (dashed lines)

When compared to the prediction from Mikielewicz and Moszynski (1976) [7], the calculation results of the present model are characterized by higher values of both the critical thickness δ_b and the stable rivulet wetting ratio X_b. This directly means that the film rupture is predicted at a higher Reynolds than the model by Mikielewicz and Moszynski (1976) [7], but at that condition the rivulet would cover about 90% of the plain wall width λ (Figure 2).

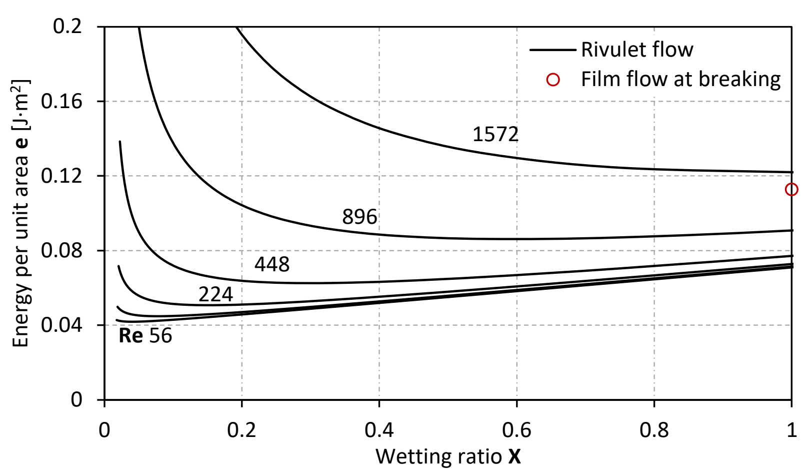

Figure 3: Specific energy [J·m^{-2}] vs wetting ratio diagram for water at 30°C

When the wetting ratio X is taken as the primary independent parameter, Figure 3 shows that, in accordance with the principle of minimum energy, the stable rivulet configuration is a condition characterized by minimal energy. The path identified by all these minima defines the stable wetting behavior of the fluid for the considered range of flow rates.

2.2 Transient Wetting Behavior

The previous section presented the criterion for establishing the critical condition at which the rupture of the film occurs and describes the stable configuration of the rivulet in terms of wetting ability X. However, the main obvious feature observable in experimental investigations is related to the gradual transition from the transversal width imposed at the distributor to a stable rivulet configuration, with a minimal and approximately constant width (Figure 4). Accordingly, in order to properly estimate the wetting behavior of thin films over plain inclined surfaces, a generalized method able to assess this transition is needed. The modeling approach followed in this section combines a Lagrangian approach for predicting the local evolution of the rivulet's wetting ability towards the stable (and steadily maintained) rivulet configuration and the previously presented energy minimization method for the identification of the latter; when writing the rivulet's Lagrangian function, the flow is assumed to be irrotational and uniquely determined by a single generalized wetting coordinate and its time derivative, which tends to zero at infinity. In parallel, the phenomenological observations and quantitative evaluation of the wetting ability of the liquid flow along a solid aluminum surface within a dedicated experimental test section (schematically illustrated in Figure 4, Trinuruka et al., 2018 [11]) are taken as a reference for a first validation and model refinements.

Figure 4: Flow visualization on a vertical aluminum wall

The evolution of the rivulet wetting ability under a forced fluid distribution width, is approximated by assuming that this transient behavior can be described by a single generalized coordinate X (and velocity $\dot{X}$), under the effect of a generalized force associated to a scalar potential Y (Eq. 22). This is defined as the energy difference between the steady rivulet configuration (associated by definition to the energy minimum) ($X\infty$, $R\infty$ and $Z\infty$) and the rivulet at time t (or stream-wise position $x \approx u_{av} \cdot t$). Finally, its wetting behavior $X(t)$ is obtained from the numerical approximation of the Lagrange equation. Due to an ideally functioning distributor at the initial stream-wise position (x=0), the rivulet is assumed to cover completely the transversal extension of the surface $X(0)$=1 and its cross-section shape ($R(t)$ and $Z(t)$) can be determined by the continuity relation (Eq. 15) and Eq. 12. The energy associated to this configuration can be calculated with reference to Eq. 17 and can be visualized on the extreme right-hand side of the graph represented in Figure 3. Similarly, for the subsequent stream-wise positions, these quantities uphold the same fundamental relations (Eqs. 15-16), whereas the local wetting ratio is assessed with reference to the numerical integration of the Lagrange equation (Eq. 26). The Lagrangian function Λ characterizing the rivulet configuration (Eq. 21) is defined by the difference of the related kinetic energy e_k (per unit stream-wise length dx and unit width λ) defined through the generalized variable X (Eq. 23), and the potential energy Y (defined in Eq. 22).

$$\Lambda = e_k(X,t) - Y(X,t) \tag{21}$$

$$Y(X,t) = e_{riv}(X,t) - e_{riv}(X_\infty) \tag{22}$$

$$e_k(\dot{X},t) = \frac{1}{2}\frac{M_{riv}}{dx\lambda}\lambda^2 \dot{X}^2 = \frac{1}{2}m_{riv}\lambda^2 \dot{X}^2 \tag{23}$$

Where m_{riv} can be calculated given the cross-sectional shape of the rivulet.

$$m_{riv} = \frac{1}{\lambda}\int_A \rho dA = \frac{\rho\left[\frac{R^2}{4}\left(\theta_0 - \sin\theta_0\right) + ZR\left(1-\cos\theta_0\right)\right]}{\lambda} \tag{24}$$

The total rate per unit area of the viscous dissipation of energy F is introduced by writing Rayleigh's dissipation integral (Eq. 25) (Harper, 2001 [12]) and incorporating it into the Lagrange equation.

$$F = \frac{1}{2}\lambda^2 \mu \frac{\lambda}{\lambda dx}\dot{X}^2 \tag{25}$$

Consequently, the Lagrange equation reduces to the formulation expressed in Eq. 26.

$$\frac{d}{dt}\left(\frac{\partial \Lambda}{\partial \dot{X}}\right) + \frac{\partial F}{\partial \dot{X}} - \frac{\partial \Lambda}{\partial X} = 0 \tag{26}$$

3. RESULTS

The numerical approximation of Eq. 26 gives the local wetting behavior of the rivulet flow (Figure 5), which can be used for a detailed appraisal of the wetted area of the solid surface.

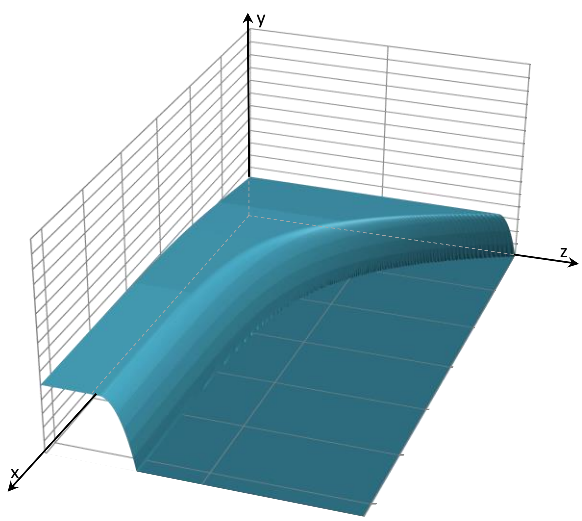

Figure 5: Calculation results for the gradual transition from uniform film to the stable rivulet configuration

3.1 Comparison with Experiments

The results obtained can be compared with the experimental results obtained from a dedicated test section (Trinuruk et al., 2018 [11]). In Figure 6 the wetting behavior of the rivulet predicted by this model formulation is qualitatively compared to the direct visualization of a water flow with corresponding flowrates. Although the local wetting behavior shows notable differences with respect to the simulated transient rivulet shape, the estimated wetting ability exhibit closely similar overall surface wetting values (as highlighted in section 3.2). The main discrepancies between simulated and experimental wetting behavior can be related to the waviness and complexity of the real hydrodynamic characteristics of the rivulet or to additional deviations between estimated and real contact angles.

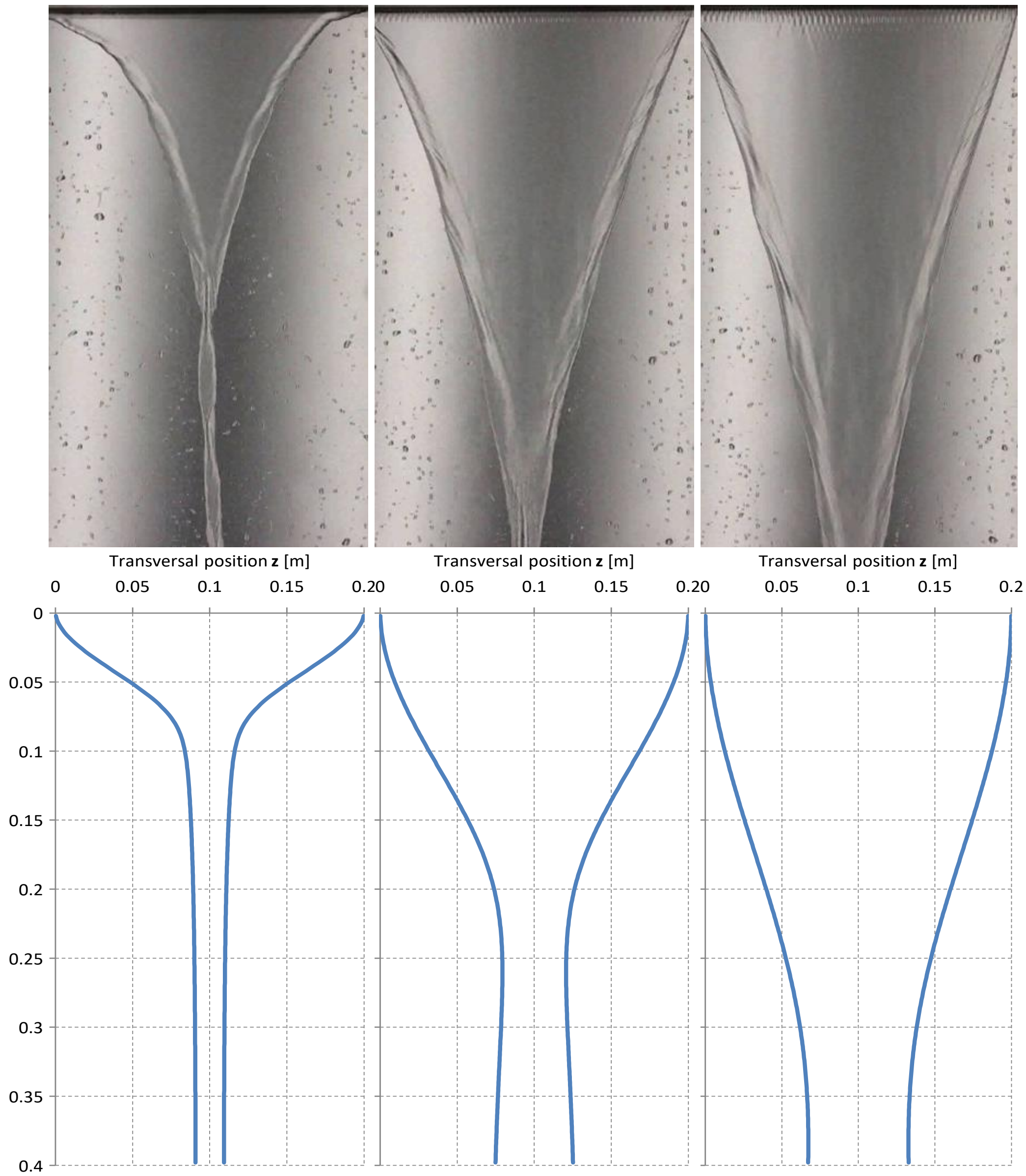

Figure 6: Qualitative comparison of the rivulet's wetting behavior of water on aluminum at *Re*≈500(a); *Re*≈1000(b); *Re* ≈1700(c)

3.2 Wetting Behavior of Falling Films over a Vertical Plain Wall

Experimentally, three different minimum wetting rates related to three different practical conditions have been distinguished in previous literature (Brauner et al., 1985 [5]): Γ_D is established when a liquid is wetting a surface which was initially completely dry, gradually increasing its mass flowrate; Γ_{Wet} is established in the same way, but

on an initially wetted surface; Γ_b occurs when the liquid flowrate is reduced to the point at which the rivulet configuration becomes stable. The last two conditions are represented by Figure 7, where, starting from a uniform film configuration, mass flowrate is reduced quasi-statically down to the film critical thickness δ_b is reached and the film breaks into the rivulet configuration. Further decreasing the mass flowrate, the rivulet reduces its extension following the path identified by the set of minimal energy configurations (blue line in Figure 7).
Since the rivulet configuration is a stable configuration, characterized by minimal energy, for quasi-statically increasing mass flowrates (i.e. Reynolds number, once the liquid properties are set constant) the rivulet configuration is maintained until the rivulet base cover the whole surface (red line in Figure 7).

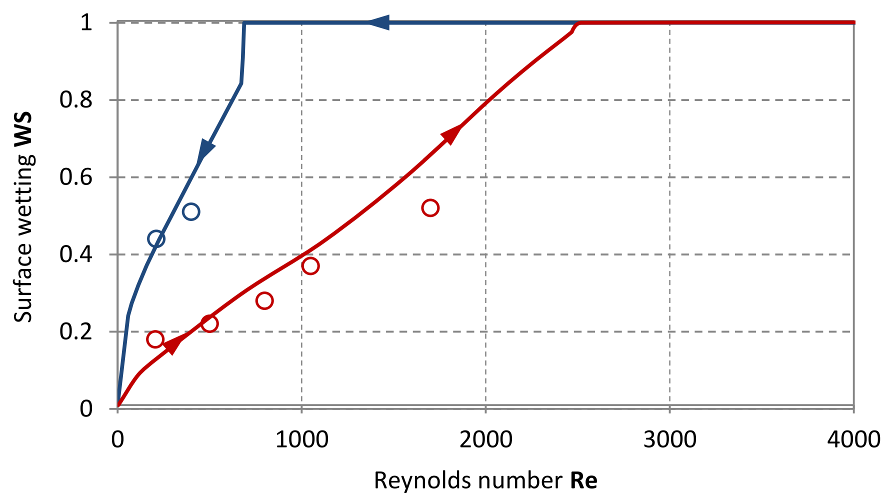

Figure 7: Wetting ratio *X* vs film Reynolds for decreasing (blue line) and increasing (red line) mass flowrates

Even though for flow rates higher than Γ_b the energy of the uniform configuration is lower than that of the rivulet configuration, the sudden change to the uniform configuration would require passing through configuration at higher energy (Figure 4). Accordingly, the values of X_∞ for increasing Reynolds correspond to the abscissa of the local minima in Figure 4, up to the condition of complete wetting (X=1, theoretically corresponding to the minimum wetting rate Γ_{Wet}). As a result, the previously presented model is able to make evidence for the wetting hysteresis behavior of falling film (Figure 6). Where, for the result calculations advancing and receding values of the contact angle have been used, respectively, when tracing red and blue lines.

4. CONCLUSIONS

A theoretical model, based on the Principle of minimum energy, has been developed in order to define a criterion for the film rupture condition over a flat inclined surface. By introducing an additional geometrical parameter for the cross-sectional shape of the rivulet and considering the resulting model generalizes earlier theories. Furthermore, analyzing the rivulet under a Lagrangian approach, the local wetting behavior of in its transition toward the stable configuration can be estimated. The following conclusion can be stated:
- The partial wetting model and the critical condition show both qualitative and quantitative agreement with experiments.
- The hysteresis phenomenon of the wetting behavior with respect to decreasing and increasing mass flow-rates can be modeled and estimated.
- This methodology is extended to include the contact angle hysteresis

As a result, the present theory can be combined with heat and mass transfer models for an enhanced characterization of transfer processes performed by using thin liquid films.

NOMENCLATURE

Nomenclature			e	Energy per unit surface	$(J\cdot m^{-2})$
A	Cross-sectional area	(m^2)	E	Energy per unit stream-wise length	$(J\cdot m^{-1})$

F	Rayleigh's dissipation integral	$(J{\cdot}m^{-2})$
g	Gravity	$(m{\cdot}s^{-2})$
L	Lagrangian function	$(J{\cdot}m^{-2})$
m	Mass per unit area	$(kg{\cdot}m^{-2})$
M	Mass	(kg)
R	Rivulet Radius	(m)
Re	Reynolds Number	
S	Interface contour	(m)
t	Time	(s)
u	Stream-wise Velocity	$(m{\cdot}s^{-1})$
x	Stream-wise position	(m)
X	Local wetting ratio	
y	Normal position	(m)
Y	Potential energy per unit area	$(J{\cdot}m^{-2})$
z	Transversal position	(m)
Z	Straight segment of the rivulet	(m)

Greek Symbols

β	Surface Inclination Angle	(rad)
Γ	Mass Flow rate per unit Width	$(kg{\cdot}m^{-1}s^{-1})$
δ	Thickness	(m)
θ	Angular position	(rad)
θ_0	Contact Angle	(rad)
λ	Solid surface Width	(m)
μ	Dynamic viscosity	$(Pa{\cdot}s)$
ρ	Density	$(kg{\cdot}m^{-3})$
σ	Surface tension	$(J{\cdot}m^{-2})$
Λ	Lagrangian function	$(J{\cdot}m^{-2})$

Subscripts

∞	Stable rivulet configuration
av	Average
b	Film rupture
D	Wetting
g	Gas
l	Liquid
k	Transversal kinetic energy
riv	Rivulet
s	Solid
σ	Surface
K	Stream-wise kinetic energy
u	Uniform film
Wet	Rewetting

REFERENCES

[1] Giannetti N., Rocchetti A., Yamaguchi S., Saito K., (2017), Analytical solution of film mass-transfer on a partially wetted absorber tube, International Journal of Thermal Sciences, Vol. 118, pp. 176-186.

[2] Giannetti N., Rocchetti A., Yamaguchi S., Saito K., (2018), Heat and mass transfer coefficients of falling-film absorption on a partially wetted horizontal tube, International Journal of Thermal Sciences, Vol. 126, pp. 56-66.

[3] Varela R.J., Giannetti N., Yamaguchi S., Saito K., Wang X.M., Nakayama H., (2018), Experimental investigation of the wetting characteristics of an aqueous ionic liquid solution on an aluminum fin-tube substrate, International Journal of Refrigeration, ACCEPTED on 18/02/2018, JIJR3901.

[4] Maron D.M., Ingel G., Brauner N., (1982), Wettability and break-up of thin films on inclined surfaces with continuous and intermittent feed, Desalination, Vol. 42, pp. 87-96.

[5] Brauner N., Maron D.M., Harel Z., (1985), Wettability, Rewettability and breakdown of thin films of aqueous solutions, Desalination, Vol. 52, pp. 295-307.

[6] Bertola V., Cafaro E., (2008), A critical analysis of the minimum entropy production theorem and its application to heat and fluid flow, International Journal of Heat and Mass Transfer, Vol. 51, pp. 1907-1912.

[7] Mikielewicz J., Moszynski J.R., (1976), Minimum thickness of a liquid film flowing vertically down a solid surface, International Journal of Heat and Mass Transfer, Vol. 19, pp. 771-776.

[8] Giannetti N., Yamaguchi S., Saito K., (2016), Wetting behavior of a liquid film on an internally-cooled desiccant contactor, International Journal of Heat and Mass Transfer, Vol. 101, pp. 958–969.

[9] Doniec A., (1988), Flow of a laminar liquid film down a vertical surface, Chemical Engineering Science, Vol. 43 (4), pp. 847-854.

[10] Doniec A., (1991), Laminar flow of a rivulet down a vertical solid surface, The Canadian Journal of Chemical Engineering, Vol. 69, pp. 198-202.

[11] Trinuruka P., Giannetti N., Kaneko T., Yamaguchi S., Saito K., (2018), Influence of the fluid distribution width on wettability and rivulet flow over vertical flat surfaces, 17th International Refrigeration and Air Conditioning Conference; Herrick Conferences, Purdue University, West Lafayette, U.S.A.

[12] Harper J.F., (2001), A Bubble Rising in Viscous Fluid: Lagrange's Equations for Motion at A High Reynolds Number. In: King A.C., Shikhmurzaev Y.D. (eds) IUTAM Symposium on Free Surface Flows. Fluid Mechanics and Its Applications, Vol. 62. Springer, Dordrecht.